# Hyaluronated liposomes containing H2S-releasing doxorubicin are effective against P-glycoprotein-positive/doxorubicin-resistant osteosarcoma cells and xenografts

# Hyaluronated liposomes containing H2S-releasing doxorubicin are effective against P-glycoprotein-positive/doxorubicin-resistant osteosarcoma cells and xenografts

Elena Gazzano[a,1], Ilaria Buondonno[a,1], Alessandro Marengo[b], Barbara Rolando[b], Konstantin Chegaev[b], Joanna Kopecka[a], Simona Saponara[c], Matteo Sorge[d], Claudia Maria Hattinger[e], Alberto Gasco[b], Roberta Fruttero[b], Mara Brancaccio[d], Massimo Serra[e], Barbara Stella[b], Elias Fattal[f], Silvia Arpicco[b,*,2], Chiara Riganti[a,**,2]

[a] *Department of Oncology, University of Torino, Torino, Italy*
[b] *Department of Drug Science and Technology, University of Torino, Torino, Italy*
[c] *Department of Life Sciences, University of Siena, Siena, Italy*
[d] *Department of Molecular Biotechnology and Health Sciences, University of Torino, Torino, Italy*
[e] *IRCCS Istituto Ortopedico Rizzoli, Laboratory of Experimental Oncology, Pharmacogenomics and Pharmacogenetics Research Unit, Bologna, Italy*
[f] *Institut Galien Paris-Sud, CNRS, Université Paris-Sud, Université Paris-Saclay, Châtenay-Malabry, France*

A B S T R A C T

Doxorubicin (dox) is one of the first-line drug in osteosarcoma treatment but its effectiveness is limited by the efflux pump P-glycoprotein (Pgp) and by the onset of cardiotoxicity. We previously demonstrated that synthetic doxs conjugated with a H2S-releasing moiety (Sdox) were less cardiotoxic and more effective than dox against Pgp-overexpressing osteosarcoma cells. In order to increase the active delivery to tumor cells, we produced hyaluronic acid (HA)-conjugated liposomes containing Sdox (HA-Lsdox), exploiting the abundance of the HA receptor CD44 in osteosarcoma.

HA-Lsdox showed favorable drug-release profile and higher toxicity *in vitro* and *in vivo* than dox or the FDAapproved liposomal dox Caelyx® against Pgp-overexpressing osteosarcoma, displaying the same cardiotoxicity profile of Caelyx®. Differently from dox, HA-Lsdox delivered the drug within the endoplasmic reticulum (ER), inducing protein sulfhydration and ubiquitination, and activating a ER stress pro-apoptotic response mediated by CHOP. HA-Lsdox also sulfhydrated the nascent Pgp in the ER, reducing its activity. We propose HA-Lsdox as an innovative tool noteworthy to be tested in Pgp-overexpressing patients, who are frequently less responsive to standard treatments in which dox is one of the most important drugs.

## 1. Introduction

Pre- and post-operative chemotherapy is the usual treatment for high grade osteosarcoma (tumor localized in the axial skeleton, metastatic at clinical onset, arisen in patients younger than 40 years). The most widely used treatment in this setting is based on the surgical removal of primary tumor combined with systemic pre- and post-operative chemotherapy based on doxorubicin (dox), methotrexate and cisplatin.

Chemotherapy is also an important component of the treatment for metastatic osteosarcoma [1–3]. Despite this aggressive multimodal approach, 35–40% of patients poorly respond to treatment and relapse.

This behavior is frequently associated with the overexpression at diagnosis of the ATP binding cassette B1/P-glycoprotein (ABCB1/Pgp), which efflux dox [4,5] and is a negative prognostic factor in osteosarcoma patients [6–9]. A second reason is the onset of dox-related cardiotoxicity that limits the cumulative dose of the drug administered [10]. The FDA-approved liposomal formulation of dox, Caelyx®, that significantly reduced the cardiotoxicity, was well-tolerated but it did not display an anti-tumor activity superior to dox in sarcoma [11,12], likely because it is no more effective than dox in Pgp-positive tumors [13,14].

Notwithstanding the multiple strategies adopted, the prognosis of patients with osteosarcoma has not significantly improved in the last years [3].

Recently, we synthesized a library of hydrogen sulfide (H2S)-releasing doxorubicins that did not elicit any cardiotoxic effect but still retained their efficacy *in vitro* on U-2OS and Saos-2 cells-derived variants characterized by increasing levels of Pgp and resistance to dox [15,16]. The lead compound, *i.e*. compound **10** in Chegaev [15], here termed Sdox, was also effective against dox-resistant prostate tumor xenografts [17].

With the goals of improving the tumor-to-healthy tissues delivery, and increasing Sdox stability and solubility, the aim of the present work was to produce and validate Sdox liposomal formulations conjugated with hyaluronic acid (HA) moiety (HA-Lsdox). Of note, the HA-receptor CD44 is expressed in osteosarcoma [18], where it promotes tumor growth and metastatic dissemination [19–22]. CD44 silencing improves the response to dox and cisplatin [23], although the molecular mechanisms are completely

unknown. The abundancy of CD44 in osteosarcoma makes it an ideal target to increase the delivery of HA-Lsdox towards the tumor. The use of a liposomal formulation similar to Caelyx® is expected to reduce cardiotoxicity. The use of Sdox instead of dox as cargo drug should guarantee good efficacy against dox-resistant/Pgp-overexpressing osteosarcoma and low cardiotoxicity. We exploited all these features to test the efficacy and safety of HA-Lsdox, and to investigate the molecular mechanisms of its anti-tumor effects in preclinical models of dox-resistant osteosarcoma.

## 2. Material and methods

### *2.1. Materials and instruments*

Sodium hyaluronate of MW 14,800 Da was purchased from Lifecore Biomedical (Chaska, MN). All the phospholipids were provided by Avanti Polar-Lipids distributed by Spectra 2000 (Rome, Italy). Cholesterol, dox and all the other chemicals were obtained from Sigma Chemicals Co. (St. Louis Mo). Plasticware for cell cultures was from Falcon (Becton Dickinson, Franklin Lakes, NJ). Foetal bovine serum (FBS) and culture medium were supplied by Invitrogen Life Technologies (Carlsbad, CA). The synthesis of Sdox was performed as described in Chegaev [15]. Conjugate between 1,2-dipalmitoyl-*sn*-glycero-3-phosphoethanolamine (DPPE) and HA (HA-DPPE) was prepared using the method described in Arpicco [24]. Reverse phase-high pressure liquid chromatography (RP-HPLC) analysis was performed as described in Chegaev [15]. Differential scanning calorimetry (DSC) was performed using a Q200 DSC (TA Instruments, New Castle, DE).

### *2.2. Preparation of liposomes*

Lsdox was prepared using the thin lipid film-hydration method mixing together chloroform solutions of 1,2-distearoil-*sn*-glycero-3-phosphocoline (DSPC), cholesterol (CHOL) and 1,2-distearoyl-*sn*-glycero-3-phosphoethanolamine-N-[amino (polyethylene glycol)-2000] (mPEG2000-DSPE) in 75:19:6M ratio and Sdox (11% ratio mol drug/mol lipid). The mixture was then evaporated by rotary evaporator and dried under vacuum overnight. The resulting lipid film was hydrated with a 20 mM 4-(2-hydroxyethyl)piperazine-1-ethanesulforic acid (HEPES) buffer (pH 7.4), the suspension was vortex-mixed for 10 min and bath sonicated. The formulations were then sequentially extruded (Extruder, Lipex, Vancouver, Canada) through 400 and then 200 nm polycarbonate membrane (Costar, Corning Incorporated, NY) at a set temperature of 5 °C above the phase transition temperature of the lipid mixture. Liposomal preparations were purified from non-encapsulated Sdox through chromatography on Sepharose CL-4B columns, eluting with HEPES buffer at room temperature. Liposomes were stored at 4 °C.

To prepare HA-Lsdox, the same method of preparation was used and the lipid film was hydrated using a solution of HA-DPPE conjugate (3 molar ratio) in HEPES buffer.

### *2.3. Liposomes characterization*

The mean particle size and polydispersity index (PDI) of the liposomes were determined at 20 °C by Dynamic Light Scattering using a Zetasizer (Nano-ZS, Malvern instruments, UK). Size measurements were performed at a fixed angle of 173° after dilution of the liposome suspensions in MilliQ® water. The surface charge of liposomes was evaluated by zeta potential measurements after dilution of the suspensions in 10 mM KCl. Phospholipid phosphorous was assessed in each liposome preparation by phosphate assay after destruction with perchloric acid [25]. The amount of encapsulated Sdox was determined by RPHPLC [14,15]. Liposomal preparations were analyzed for physical stability in the storage conditions (4 °C) and for Sdox release in FBS and HEPES buffer at 37 °C as previously reported in Pedrini [26]. Briefly, to evaluate Sdox release in FBS, the formulations were diluted 1:2.5 with FBS and incubated at 37 °C for various periods of time; drug leakage was determined submitting 200 μL of liposomes to purification through chromatography on Sepharose CL-4B columns. Then, the drug and lipid content was measured in the collected liposomal fractions and compared with initial values. For comparison, a drug leakage study was also performed in HEPES buffer at 37 °C.

For DSC analysis about 15 mg of hydrated samples suspension were introduced into a 40 μl aluminium pan and analyzed. DSC runs were conducted from 25 °C to 80 °C at a rate of 5 °C/min under constant nitrogen stream (50 ml/min). The main transition temperature (Tm) was determined as the onset temperature of the highest peak.

### *2.4. Cells*

Murine dox-resistant osteosarcoma K7M2 cells, human dox-sensitive osteosarcoma U-2OS were purchased from ATCC (Manassas, VA).
The corresponding dox-resistant variant U-2OS/DX580, selected by culturing parental cells in a medium with 580 ng/ml dox, was generated as reported in Serra [27], and continuously cultured in presence of dox. Cells were maintained in DMEM supplemented with 10% v/v FBS, 1% v/v penicillin-streptomycin, 1% v/v L-glutamine.

*2.5. Immunoblotting*

20 μg of protein extracts were subjected to 4–20% gradient SDSPAGE and probed with the following antibodies: anti-ABCB1/Pgp (Merck Millipore, Burlington, MA); anti-CD44 (Abcam, Cambridge, UK); anti–CAATenhancer-binding protein-β (C/EBP-β, Santa Cruz Biotechnology Inc., Santa Cruz, CA), anti-C/EBP homologous protein/growth arrest and DNA damage 153 (CHOP/GADD153, Santa Cruz Biotechnology Inc.), anti-Tribbles homolog 3 (TRB3, Proteintech, Chicago, IL), anti-p53 up-regulated modulator of apoptosis (PUMA, Cell Signaling Technology, Danvers, MA); anti-caspase 12 (Abcam), anticaspase 7 (Abcam), anti-caspase 3 (GeneTex, Hsinhu City, Taiwan), anti-β-tubulin (Santa Cruz Biotechnology Inc.), followed by peroxidaseconjugated secondary antibodies (Bio-Rad Laboratories, Hercules, CA).
Microsomal fractions were prepared using the Endoplasmic Reticulum Isolation Kit (Sigma Chemicals. Co), as per manufacturer's instructions. 100 μg of microsomal proteins were probed with the anti-Pgp antibody or with an anti-calreticulin antibody (Affinity Bioreagents, Rockford, IL). To measure ubiquitinated Pgp, 50 μg of microsomal proteins were immunoprecipitated with the anti-Pgp antibody, using 25 μl of PureProteome Magnetic Beads (Millipore), then probed with an antimono/poly-ubiquitin antibody (Axxora, Lausanne, Switzerland).

*2.6. Flow cytometry*

1×106 cells were rinsed and fixed with 2% w/v paraformaldehyde (PFA) for 2 min, washed three times with PBS and stained with the anti-CD44 antibody (Abcam) for 1 h on ice, followed by an AlexaFluor 488-conjugated secondary antibody (Millipore) for 30 min. 1×105 cells were analyzed with EasyCyte Guava™ flow cytometer (Millipore), equipped with the InCyte software (Millipore). Control experiments included incubation with non-immune isotype antibody.

*2.7. Intracellular and subcellular doxorubicin accumulation*

Dox content in whole cell lysates, in nuclear and microsomal fractions - isolated with the Nuclear Extract kit (Active Motif, La Hulpe, Belgium) and the Endoplasmic Reticulum Isolation Kit (Sigma Chemicals. Co), respectively - was measured fluorimetrically [28].
Subcellular localization of Sdox was measured by fluorescence microscope as reported in Buondonno [16].

*2.8. Cytotoxity, apoptosis and cell viability*

The extracellular release of lactate dehydrogenase (LDH), considered an index of cell damage and necrosis, was measured as reported in Riganti [28]. The activation of caspase 3, an index of apoptosis, was measured fluorimetrically as detailed in Riganti [29]. Cell viability was measured by the ATPlite Luminescence Assay System (PerkinElmer, Waltham, MA), as per manufacturer's instructions.

*2.9. In vivo tumor growth*

1×107 K7M2 cells, re-suspended in 100 μl Matrigel, were subcutaneously implanted in 6-week old female Balb/C mice. Tumor volume was monitored by caliper and calculated according to the equation: (LxW2)/2, where L=tumor length and W=tumor width. When tumor reached the volume of 50 mm3, animals were randomized and treated as reported in Fig. 2. Tumor volumes were monitored daily by caliper and animals were euthanized at day 21 after randomization with zolazepam (0.2 ml/kg) and xylazine (16 mg/kg). Tumors were collected and photographed, then homogenized for 30 s at 15 Hz, using a TissueLyser II device (Qiagen, Hilden, Germany) and clarified at 12,000×g for 5 min. 10 μg of proteins from tumor lysates were used for the immunoblot analysis of CD44, Pgp and caspase 3, as reported above. In a cohort of mice, tumors before randomization and at the end of the treatments were excised, digested by mechanical dissociation followed by 1 h incubation in complete culture medium containing 1 mg/ml collagenase and 0.2 mg/ml hyaluronidase at 37 °C, then centrifuged at 12,000×g for 5 min, plated in fresh medium and tested for their chemosensitivity 24 h after re-plating. The hematochemical parameters were measured on 0.5 ml of blood collected immediately after mice sacrifice, using the respective kits from Beckman Coulter Inc.(Miami, FL). Hearts were fixed in 4%

v/v paraformaldehyde. The paraffin sections were stained with hematoxylin/eosin, with picrosirius red solution to detect fibrotic tissue [30] and with wheat germ agglutinin-Alexa Fluor™ 488 conjugate (Molecular Probes, Eugene, OR) to evaluate cardiomyocyte area [14]. Sections were examined with Leica Olympus provis AX70 microscope (Leica Microsystems GmbH, Wetzlar, Germany; 10 x ocular lens, 20–40 x objective, depending on the assay) and Nikon Eclipse 80i-ViCO microscope (Nikon Corporation, Tokyo, Japan; 10x ocular lens, 40 x objective).

Animal care and experimental procedures were approved by the Bio-Ethical Committee of the Italian Ministry of Health (#122/2015-PR).

*2.10. PCR arrays*

Total RNA was extracted and reverse-transcribed using iScript™ cDNA Synthesis Kit (Bio-Rad Laboratories). The PCR arrays were performed on 1 μg cDNA, using the Unfolded Protein Response Plus PCR Array (Bio-Rad Laboratories), as per manufacturer's instructions. Data analysis was performed with PrimePCR™ Analysis Software (Bio-Rad Laboratories).

*2.11. Protein sulfhydration*

The sulfhydration of microsomal proteins (100 μg) or immunopurified Pgp (50 μg) was measured according to Sen [31].

*2.12. Protein ubiquitination*

The ubiquitination of microsomal proteins (100 μg) or immunopurified Pgp (50 μg) was measured with the E3Lite Customizable Ubiquitin Ligase kit (Life-Sensors Inc., Malvern, PA), as detailed in Buondonno [16].

*2.13. Pgp ATPase activity*

The Pgp ATPase activity was measured in Pgp-rich membrane vesicles as described in Kopecka [32].

*2.14. Cell silencing*

2×105 cells, seeded in 0.25 ml FBS/antibiotic-free medium, were transfected either with non-targeting scrambled siRNA pools or siRNA pools targeting CHOP/GADD53 (target sequences: NM_001290183.1; NM_007837.4; ThermoScientific), as per manufacturer's protocol. The efficacy of silencing was verified by immunoblotting 48 h after the transfection.

*2.15. Statistical analysis*

All data in the text and figures are provided as means ± SD. The results were analyzed by a one-way analysis of variance (ANOVA) and Tukey's test. $p < 0.05$ was considered significant.

## 3. Results

*3.1. Liposomes formulation and characterization*

Lsdox and HA-Lsdox were prepared by hydration of the drug-lipid film followed by extrusion through polycarbonate filters to obtain homogenous small unilamellar vesicles. HA-Lsdox were prepared by adding the HA-DPPE conjugate during the hydration phase of lipid film: in this way the phospholipidic chain was incorporated into the liposome membrane, while the HA was exposed towards the aqueous phase.

Liposomes dimensions ranged from 190 nm to 204 nm, with a slight increase in the HA-conjugated formulations. The PDI was low for all the formulations (< 0.13). The zeta potential value was negative and lower for HA-Lsdox compared to the Lsdox, due to the carboxylic negative residues of HA on the surface. The liposomes showed good and comparable Sdox entrapment efficiency, indicating that the HA-DPPE conjugate did not affect Sdox encapsulation (Table 1). After 4 weeks of storage in HEPES buffer at 4 °C all the formulations still conserved 85% of the initial Sdox content; over this period no appreciable size and/or zeta potential change, no precipitation or liposomes aggregation were observed. Lsdox and HA-Lsdox showed similar Sdox release profile in FBS and HEPES buffer at 37 °C: 50% of the compound was released after 72 h in buffer and after 48 h in serum. Nor dox neither other degradation products from encapsulated Sdox were detected.

The thermal changes caused by the incorporation of Sdox in the phospholipid bilayer were investigated by DSC (Supplementary Fig. S1; Table S1). The thermogram of pure DSPC showed the main transition peak at Tonset 54.2 °C, while with Sdox the main transition was lowered to Tonset 52.3 °C and the melting temperature peaks were broader, either in the presence of mPEG2000-DSPE and of HA-DPPE conjugate.

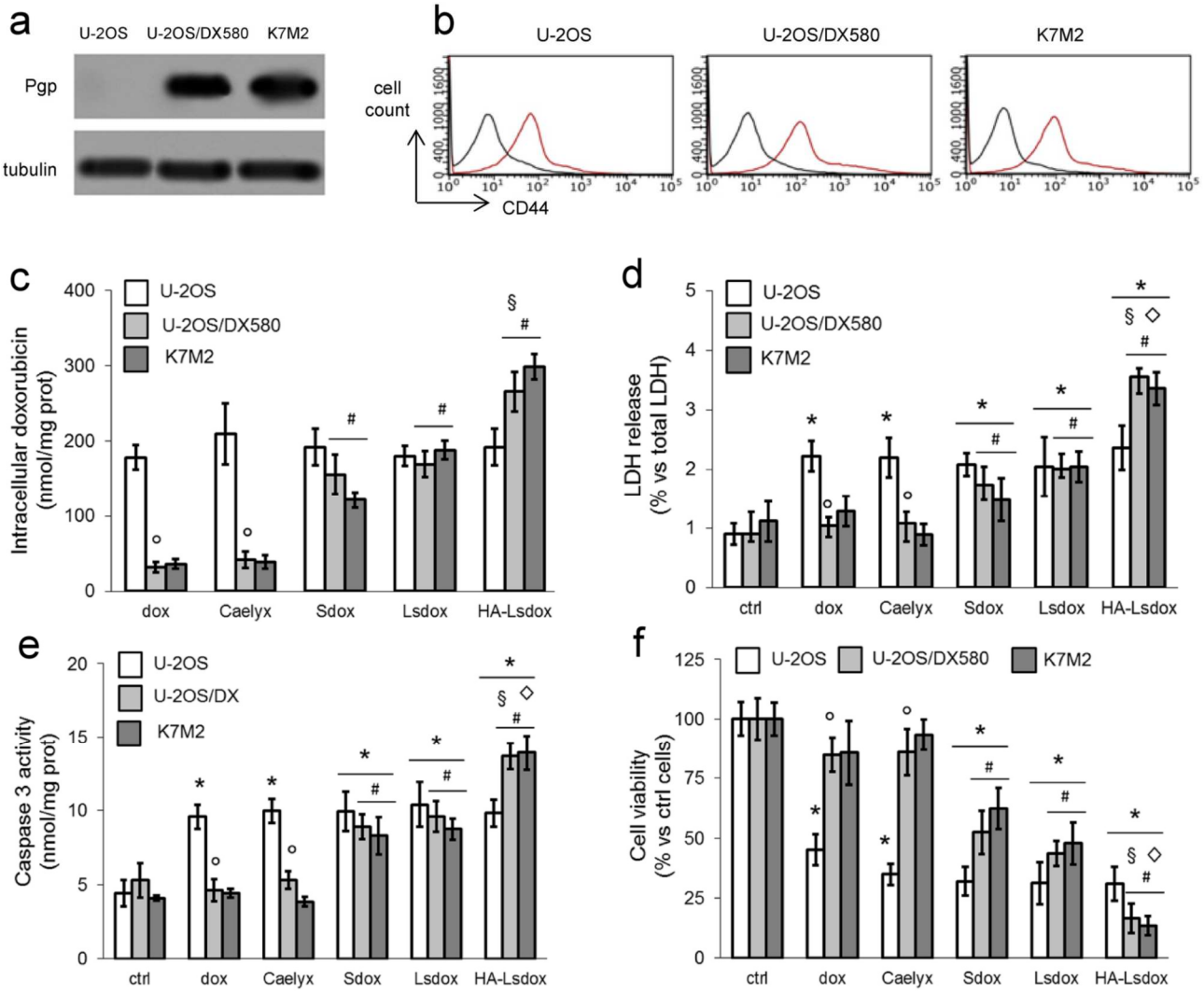


Fig. 1. **Hyaluronated liposomes containing H2S-releasing doxorubicin effectively induce cell death in doxorubicin-resistant osteosarcoma cells.**

Human doxorubicin-sensitive U-2OS, their resistant subline U-2OS/DX580 and murine doxorubicin-resistant K7M2 cells were incubated 6 h (panel c), 24 h (panels d–e) or 96 h (panels f) in fresh medium (ctrl), in medium containing 5 μM doxorubicin (dox), liposomal doxorubicin Caelyx®, H2S-releasing doxorubicin (Sdox), liposomal Sdox (Lsdox) or hyaluronated liposomal Sdox (HA-Lsdox). a. Expression of ABCB1/Pgp in untreated cells by immunoblotting. The β-tubulin expression was used as control of equal protein loading. The figure is representative of 1 out of 3 experiments. b. Surface CD44 in untreated cells, measured as per flow cytometry in duplicates. Blank: cells incubated with not-immune isotypic antibody. Histograms are representative of 1 out of 5 experiments. The percentage of CD44-positive cells as means ± SD is: 46 ± 11% (U-2OS cells); 76 ± 8% (U-2OS/DX580 cells); 69 ± 7% (K7M2 cells). *$p < 0.05$: Ue2OS/DX580 and K7M2 cells vs. U-2OS cells. c. Intracellular doxorubicin accumulation, measured by a fluorimetric assay in duplicates. Data are means ± SD (n=4 independent experiments). °$p < 0.001$: DXcells vs. parental Ue2OS cells; #$p < 0.001$: Sdox/Lsdox/HA-Lsdox vs. dox/Caelyx®; §$p < 0.002$: HA-Lsdox vs Sdox; ◊$p < 0.001$: HA-Lsdox vs Lsdox. d. Extracellular release of LDH measured spectrophotometrically in triplicates. Data are means ± SD (n = 4 independent experiments). *$p < 0.01$: treated vs. respective untreated (ctrl) cells; °$p < 0.001$: DX-cells vs. parental U-2OS cells; #$p < 0.001$: Sdox/Lsdox/HA-Lsdox vs. dox/Caelyx®; §$p < 0.001$: HA-Lsdox vs Sdox; ◊$p < 0.001$: HALsdox vs. Lsdox. e. Activation of caspase 3 measured fluorimetrically in triplicates. Data are means ± SD (n = 4 independent experiments). *$p < 0.01$: treated vs. respective untreated (ctrl) cells; °$p < 0.001$: U2OS/DX580 cells vs. parental U-2OS cells; #$p < 0.001$: Sdox/Lsdox/HA-Lsdox vs. dox/Caelyx®; §$p < 0.001$: HALsdox vs Sdox; ◊$p < 0.005$: HA-Lsdox vs Lsdox. f. Percentage of viable cells, measured by a chemiluminescence-based assay in quadruplicates. Data

are means ± SD (n = 6 independent experiments). *p < 0.01: treated vs. respective untreated (ctrl) cells; °p < 0.001: U-2OS/DX580 cells vs. parental U-2OS cells; #p < 0.05: Sdox/Lsdox/HA-Lsdox vs. dox/Caelyx®; §p < 0.001: HA-Lsdox vs. Sdox; ◊p < 0.005: HA-Lsdox vs. Lsdox.

### 3.2. *Hyaluronated liposomes containing H2S-releasing doxorubicin are effective against doxorubicin-resistant osteosarcoma in vitro and in vivo*

U-2OS and U-2OS/DX580 human osteosarcoma cell lines presenting low and high Pgp expression, respectively, and murine Pgp-expressing K7M2 (Fig. 1a) had also detectable levels of the HA receptor CD44 (Fig. 1b). CD44 levels were higher in Pgp-expressing cells. As expected dox and Caelyx® had lower intracellular accumulation (Fig. 1c). Since it is common to have a different kinetic of drug uptake and cytotoxicity between free dox and liposomal formulations [14,26], because of the slower release of dox from the liposomes, we used either short term assays (such as the release of the LDH and the activation of caspase 3 after 24 h) and long term assays (such as the measure of cell viability after 72 h), to have an in depth characterization of Sdox, Lsdox and HALsdox toxicity. Dox and Caelyx® induced lower cell damage (Fig. 1d), apoptosis (Fig. 1e) and higher viability (Fig. 1f) in U-2OS/DX580 and K7M2 cells. By contrast, Sdox, either as free drug or Lsdox was retained within Pgp-overexpressing Ue2OS/DX580 and K7M2 cells (Fig. 1c), at a sufficient amount to induce a significant damage and apoptosis, and to reduce viability (Fig. 1d–f). These effects were significantly increased using HA-Lsdox (Fig. 1c–f). Neither Sdox nor its liposomal formulations increased the efficacy of dox or Caelyx® in dox-sensitive U-2OS cells. In line with the absent efficacy in vitro, neither dox nor Caelyx® reduced the growth of K7M2 tumors (Fig. 2a and b), chosen as a prototypical example of CD44 and Pgp-overexpressing osteosarcoma (Fig. 2c), nor induced intratumor apoptosis (Fig. 2c). A progressive decrease in the rate of tumor growth paralleled by a progressive increase in the activation of intratumor caspase 3 was elicited by Sdox formulations, following this rank order: Sdox < Lsdox < HA-Lsdox (Fig. 2a–c). These agents also progressively reduced the intratumor expression of Pgp, contrarily to dox and Caelyx® (Fig. 2c).

To verify that the chemoresistant phenotype of K7M2 tumors was maintained during the whole treatment, cells obtained from excised tumors – collected before and after the treatments – were assessed for the intracellular retention of dox, Caelyx®, Sdox, Lsdox and HA-Lsdox, and for reduction of cell viability induced by each agent. As shown in the Supplementary Fig. S2a, K7M2 derived from tumors at both time points accumulated Sdox, Lsdox and HA-Lsdox at higher amounts than dox and Caelyx®, behaving like parental K7M2. Consistently, dox and Caelyx® did not reduce the viability of cells derived from the tumors, while Sdox, Lsdox and in particular HA-Lsdox did so (Supplementary Fig. S2b).

Dox, Caelyx®, Sdox and the liposomal formulations did not display signs of liver and kidney toxicity, according to the hematochemical parameters of the treated animals. As expected, dox increased CPK, CPK-MB and cTNT, indexes of cardiotoxicity, while Caelyx® did not.

Notably, Sdox, Lsdox and HA-Lsdox had a cardiotoxicity profile superimposable to Caelyx® (Supplementary Table S2). In our experimental conditions, dox did not alter cardiac tissue morphology, did not elicit fibrosis (Supplementary Fig. S3a), did not induce significant changes in cardiomyocyte cross sectional area (Supplementary Fig. S3b). Caelyx®, Sdox and its liposomal formulations did not alter these parameters as well (Supplementary Fig. S3).

**Table 1**
Characteristics of liposomes containing Sdox (means ± SD; n = 3).

| Formulation | Mean particle size (nm ± SD) | Polydispersity Index | Zeta potential (mV ± SD) | Entrapment efficiency (%)[a] |
|---|---|---|---|---|
| Lsdox | 190 ± 3 | 0.112 | −7.51 ± 0.8 | 92.8 ± 3.2 |
| HA-Lsdox | 204 ± 2 | 0.121 | −15.8 ± 1.3 | 91.3 ± 3.1 |

[a] Ratio between drug/lipid molar ratio after purification and drug/lipid molar ratio after extrusion.

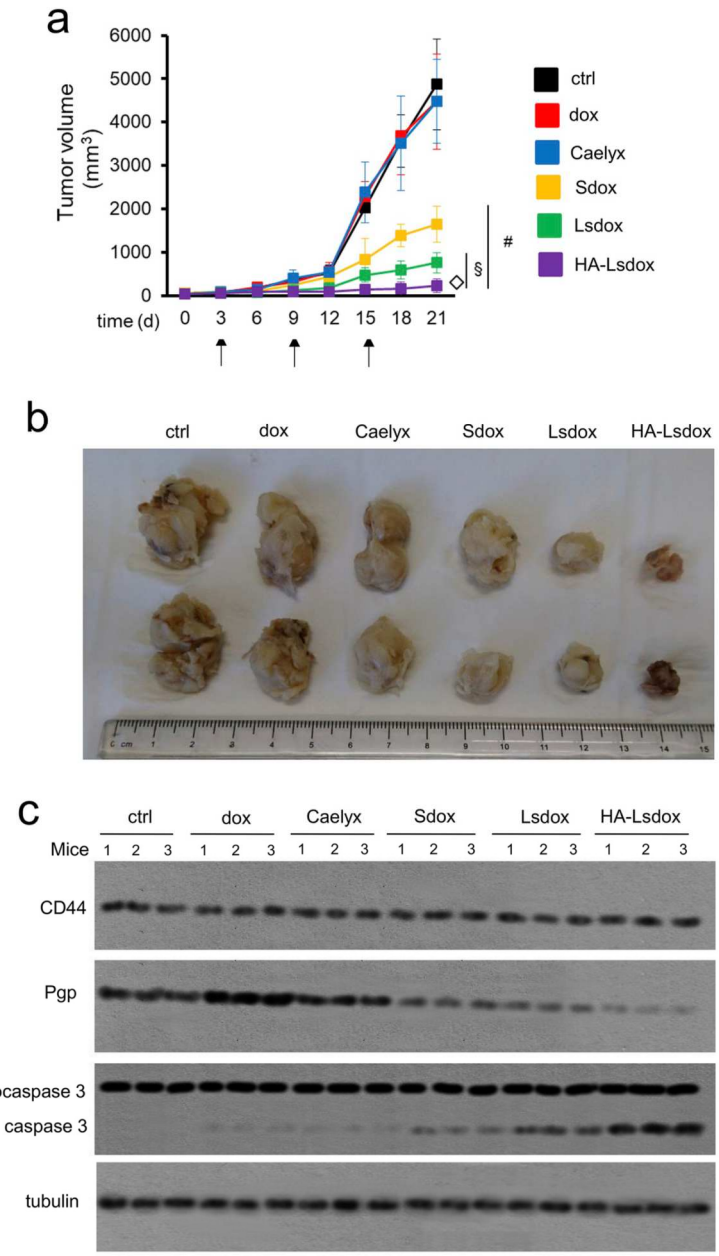


**Fig. 2. Hyaluronated liposomes containing H2S-releasing doxorubicin reduce the growth of osteosarcoma refractory to doxorubicin and Caelyx®.**

K7M2 cells were subcutaneously implanted in 6-week old female Balb/C mice. When tumor reached the volume of 50 mm3, animals were randomized in the following groups (n=8/group) and treated as it follows at day 3, 9, 15 after randomization: 1) control group, treated with 200 µl sterile physiological solution, intravenously (i.v.); 2) dox group, treated with 200 µl sterile physiological solution containing 5 mg/kg dox, i.v.; 3) Caelyx® group, treated with 200 µl sterile solution of Caelyx®, equivalent to 5 mg/kg dox, i.v.; 4) Sdox group, treated with 200 µl sterile physiological solution containing 5 mg/kg Sdox, i.v.; 5) Lsdox group, treated with 200 µl sterile solution of Lsdox, equivalent to 5 mg/kg Sdox, i.v.; 6) HA-Lsdox group, treated with 200 µl sterile solution of HA-Lsdox, equivalent to 5 mg/kg Sdox, i.v. a. Tumor growth was monitored daily by caliper measurement. Data are presented as means } SD. #$p < 0.05$: Sdox/Lsdox/HA-Lsdox vs. ctrl/dox/Caelyx®; §$p < 0.001$: HA-Lsdox vs. Sdox; ◊$p < 0.005$: HA-Lsdox vs. Lsdox (days: 15–21). b. Photographs of representative tumors of each group. c. Immublot analysis of the indicated proteins in tumor homogenates. The β-tubulin expression was used as control of equal protein loading. The figure reports the results obtained in 3 animals/group of treatment.

*3.3. Hyaluronated liposomes containing H2S-releasing doxorubicin localized within endoplasmic reticulum where they impair the ERAD/ERQC system*

Dox has a typical intranuclear localization [29], as observed in the parental U-2OS cells with low Pgp levels (Fig. 3a), but the intranuclear accumulation was dramatically reduced in Pgp-overexpressing U-2OS/DX580 and K7M2 cells (Fig. 3a). Caelyx® followed the same trend. By contrast, Sdox and its liposomal formulations showed a very low accumulation within the nucleus (Fig. 3a), while must of dox – in particular if delivered as HA-LSdox - was recovered within the microsomal fractions (Fig. 3b; Supplementary Fig. S4).

A targeted expression profile of endoplasmic reticulum-associated degradation/endoplasmic reticulum quality control (ERAD/ERQC)-related genes – that play a critical role in the folding and export of nascent proteins from the ER [33,34] – revealed that – contrarily to dox and Caelyx® – Sdox and its liposomal formulations up-regulated most of ERAD/ERQ genes in Pgp-positive K7M2 (Fig. 3c) and U-2OS/DX580 (Supplementary Fig. S5a) cells. ER-associated proteins were significantly more sulfhydrate by Sdox, Lsdox and in particular HA-Lsdox (Fig. 3d; Supplementary Fig. S5b). Such sulfhydration was paralleled by an increased ubiquitination (Fig. 3e, Supplementary Fig. S5c), likely elicited by the H2S release, since sulfhydration and ubiquitination were abrogated by the H2S scavenger hydroxycobalamin (Fig. 3d and e; Supplementary Figs. S5b–c). In line with the low retention within the ER (Fig. 3b), the gene expression profile (Fig. 3c; Supplementary Fig.S5a) and the absence of H2S-releasing groups, dox and Caelyx® did not induce sulfhydration nor ubiquitination of ER proteins in murine (Fig. 3d and e) and human (Supplementary Figs. S5b–c) resistant cells.

*3.4. Hyaluronated liposomes containing H2S-releasing doxorubicin trigger a ER-dependent apoptosis in doxorubicin-resistant osteosarcoma cells*

An increased burden of misfolded proteins within ER elicits an adaptive response known as unfolded protein response (UPR) that can overcome the stressing condition leading to cell survival or trigger cell death in case of irreversible damages [33,34]. While dox and Caelyx® did not affect the expression of UPR-related genes in K7M2 (Fig. 4a) and U-2OS/DX580 (Supplementary Fig. S6a) cells, Sdox, Lsdox and HALsdox up-regulated most UPR-sensors and effectors of UPR-mediators of cell death, while they down-regulated most UPR-mediators of cell survival (Fig. 4b; Supplementary Fig. S6b). In both murine (Fig. 4c) and human (Supplementary Fig. S6c) Pgpexpressing cells, Sdox, Lsdox and in particular HA-Lsdox increased the ER stress-sensitive isoform of C/EBP-β (i.e. C/EBP-β LIP), the proapoptotic LIP downstream effectors CHOP, TRB3 and PUMA, and induced the cleavage of caspases 12/7/3, while dox and Caelyx® were ineffective.

To prove that the C/EBP-β LIP target CHOP was critical in inducing such ER-dependent apoptosis, we transiently silenced this protein in K7M2 cells. CHOP silencing abrogated the increase of TRB3, PUMA, cleaved caspases 12, 7 and 3 in response to Sdox and HA-Lsdox (Fig. 4d), suggesting that CHOP mediated these processes in response to HA-LSdox.

*3.5. Hyaluronated liposomes containing H2S-releasing doxorubicin downregulate Pgp via sulfhydration and ubiquitination*

An intriguing effect observed in HA-Lsdox-treated tumors was the strong decrease in Pgp expression (Fig. 2c).

While dox and Caelyx® did not modify the sulfhydration (Fig. 5a) nor the catalytic activity (Fig. 5b) of Pgp isolated from the ER of K7M2 cells, Sdox, Lsdox and maximally HA-Lsdox increased Pgp sulfhydration, decreased its ATPase activity and increased Pgp ubiquitination (Fig. 5a–d). The same effects were elicited by Sdox, Lsdox and HALsdox in U-2OS/DX580, contrarily to dox and Caelyx® (Supplementary Figs. S7a–d). The release of H2S was responsible for all these processes, since hydroxycobalamin prevented the sulfhydration, the decrease in catalytic activity and the ubiquitination of Pgp (Fig. 5a–d; Supplementary Figs. S7a–d).

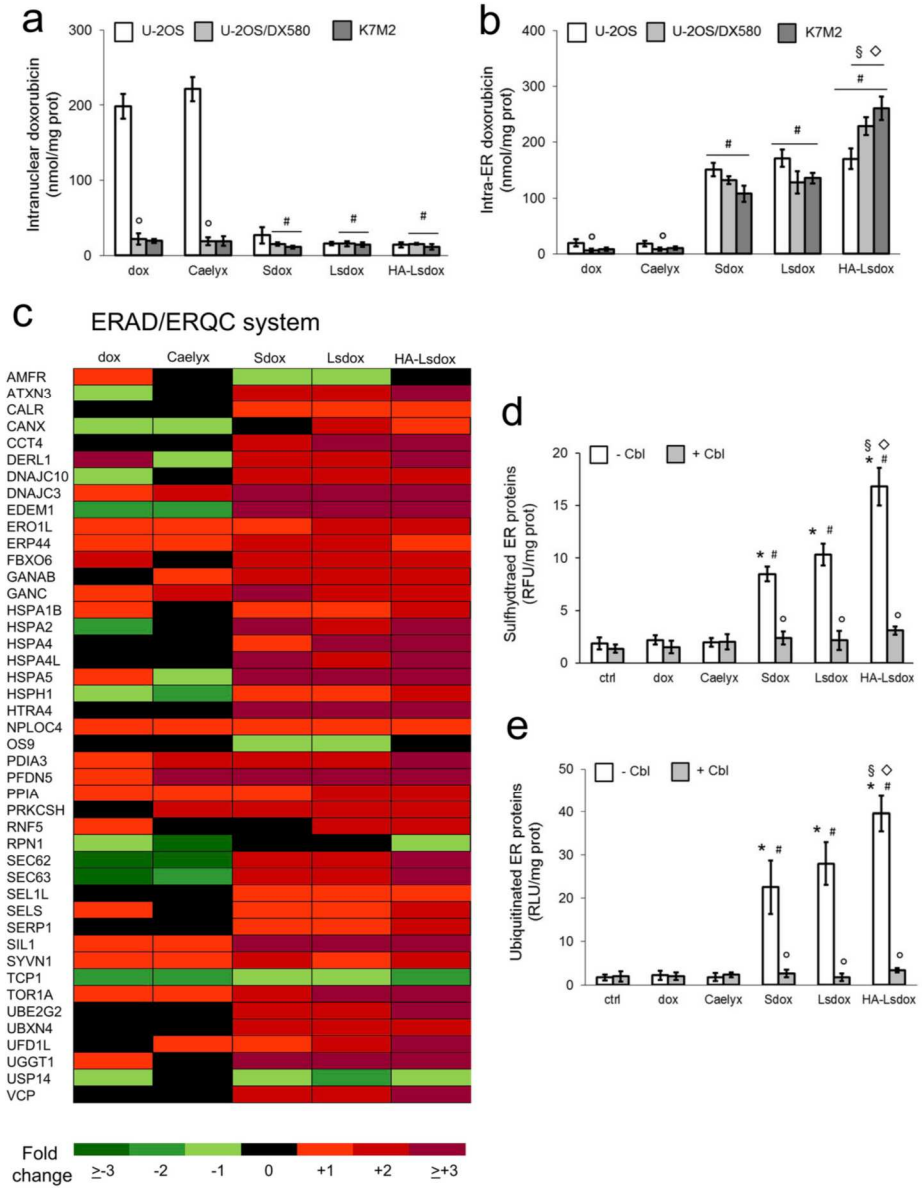


**Fig. 3. Hyaluronated liposomes containing H2S-releasing doxorubicin impair the ERAD/ERQC system of doxorubicin-resistant osteosarcoma cells. a-b.**

Human doxorubicin-sensitive U-2OS cells and their resistant subline U-2OS/DX580 cells, murine doxorubicin-resistant osteosarcoma K7M2 cells were incubated 6 h with fresh medium (ctrl), medium containing 5 μM doxorubicin (dox), liposomal doxorubicin Caelyx®, H2S-releasing doxorubicin (Sdox), liposomal Sdox (Lsdox) or hyaluronated liposomal Sdox (HA-Lsdox). After this incubation time, nuclear and microsomal fractions were extracted as reported in the Materials and Methods section. The intracellular doxorubicin accumulation was measured by a fluorimetric assay in duplicates, in nuclear (panel a) and microsomal (panel b) extracts. Data are means ± SD (n=4 independent experiments). °$p < 0.02$: DX-cells vs. parental U-2OS cells; #$p < 0.02$: Sdox/Lsdox/HA-Lsdox vs. dox/Caelyx®; §$p < 0.001$: HA-Lsdox vs. Sdox; ◊$p < 0.001$: HA-Lsdox vs. Lsdox. c. Heatmap of ER-associated degradation/endoplasmic reticulum quality control (ERAD/ERQC)-related genes in K7M2 cells, incubated as reported in a for 24 h. The figure reports genes up-or down-regulated at least two-fold compared to untreated cells, where the expression of each gene in untreated cells was considered 1 (not shown in the figure; n=6 independent experiments). d. Fluorimetric analysis of sulfhydrated microsomal proteins, performed in triplicates. When indicated, 100 μM of hydroxycobalamin (Cbl), a H2S scavenger, was co-incubated. Data are means ± SD (n = 5 independent experiments). *$p < 0.01$: treated vs. respective untreated (ctrl) cells; °$p < 0.001$: Cbl-treated cells vs. corresponding Cbl-untreated cells; #$p < 0.001$: Sdox/Lsdox/HA-Lsdox vs. dox/Caelyx®; §$p < 0.002$: HA-Lsdox vs. Sdox; ◊$p < 0.002$: HA-Lsdox vs. Lsdox. e. Ubiquitination of microsomal proteins, measured by a

chemiluminescence-based assay in triplicates, in K7M2 cells incubated as reported in d. Data are means ± SD (n=5 independent experiments). *p < 0.01: treated vs. respective untreated (ctrl) cells; °p < 0.001: Cbl-treated cells vs. corresponding Cbl-untreated cells; #p < 0.001: Sdox/Lsdox/HA-Lsdox vs. dox/Caelyx®; §p < 0.05: HA-Lsdox vs. Sdox; ◊p < 0.05: HA-Lsdox vs. Lsdox.

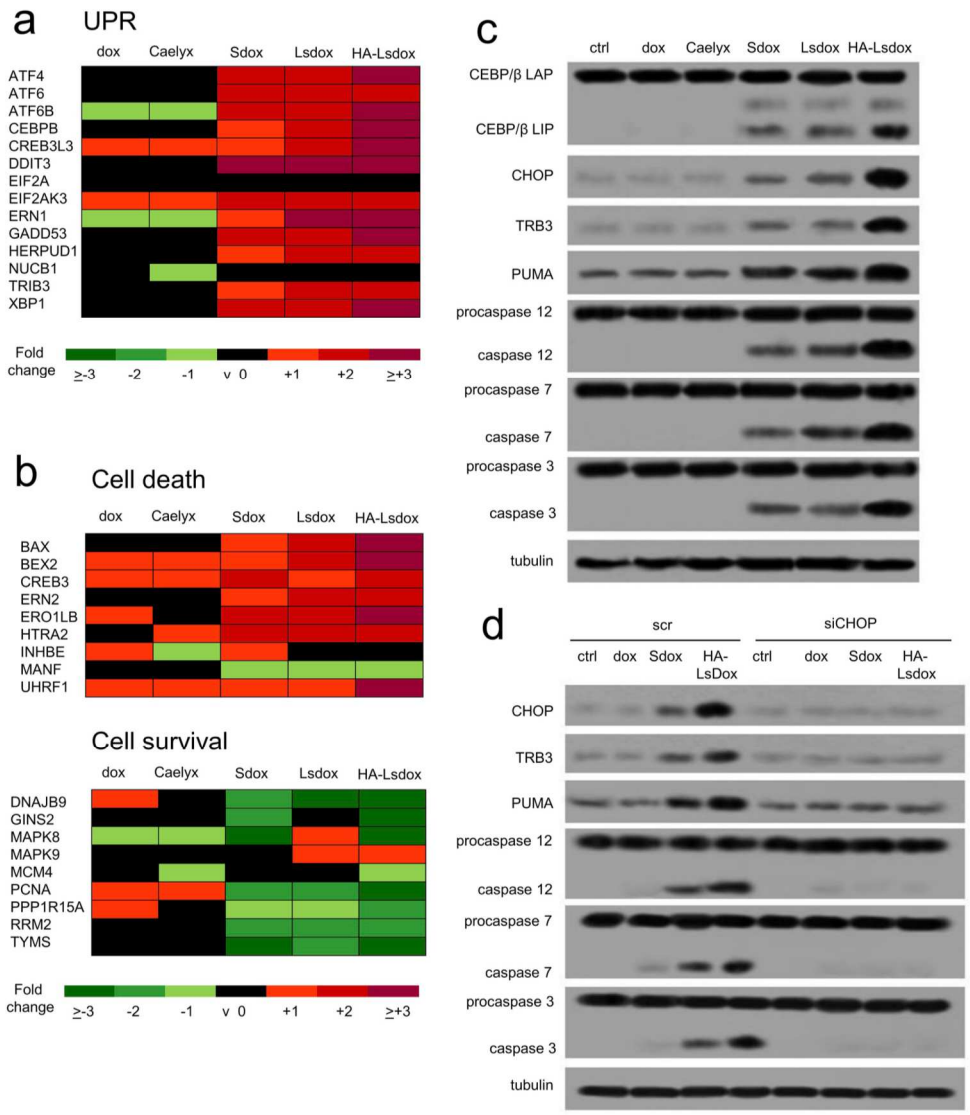


**Fig. 4. Hyaluronated liposomes containing H2S-releasing doxorubicin triggers a ER stress-dependent apoptosis in doxorubicin-resistant osteosarcoma cells**.

Murine doxorubicin-resistant osteosarcoma K7M2 cells were incubated 24 h with fresh medium (ctrl), medium containing 5 μM doxorubicin (dox), liposomal doxorubicin Caelyx®, H2S-releasing doxorubicin (Sdox), liposomal Sdox (Lsdox) or hyaluronated liposomal Sdox (HA-Lsdox). a. Heatmap of unfolded protein response (UPR)-related genes. The figure reports genes up-or down-regulated at least two-fold compared to untreated cells, where the expression of each gene in untreated cells was considered 1 (not shown in the figure; n=6 independent experiments). b. Heatmap of genes related to ER-dependent cell death or survival. The figure reports genes up-or down-regulated at least two-fold compared to untreated cells, where the expression of each gene in untreated cells was considered 1 (not shown in the figure; n=6 independent experiments). c. Cells treated as in a were lysed and probed with the indicated antibodies. The β-tubulin expression was used as control of equal protein loading. d. K7M2 cells were transfected with non-targeting scrambled siRNA pools (scr) or with siRNA pools targeting CHOP/GADD53 (siCHOP). 24 h after the transfection, the medium was changed and cells were grown for additional 24 h in fresh medium (ctrl) or in medium containing 5 μM dox, Sdox, HA-Lsdox. Whole cell lysates were probed with the indicated antibodies. The β-tubulin expression was used as control of equal protein loading. The figure is representative of 1 out of 4 experiments.

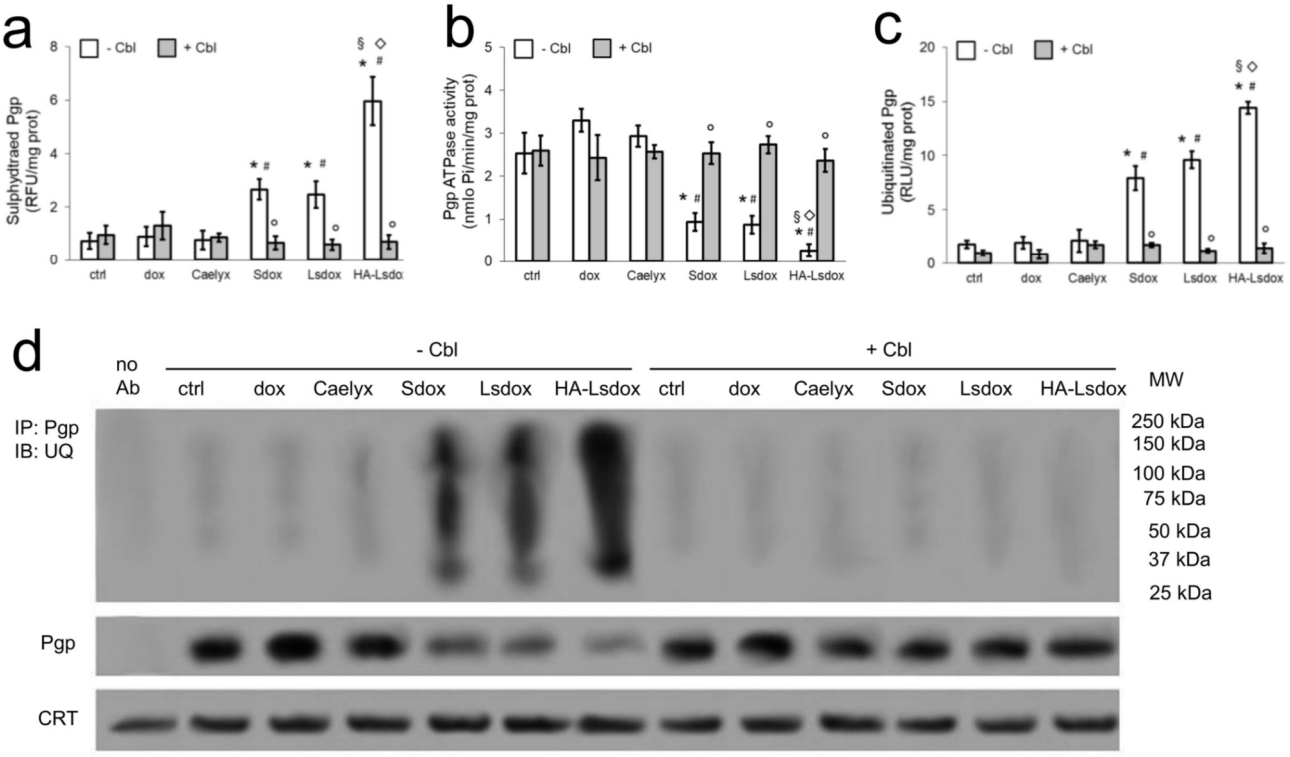


**Fig. 5. Hyaluronated liposomes containing H2S-releasing doxorubicin reduce Pgp in doxorubicin-resistant osteosarcoma cells by increasing the protein sulfhydration and ubiquitination.**

Murine doxorubicin-resistant osteosarcoma K7M2 cells were incubated 24 h with fresh medium (ctrl), medium containing 5 μM doxorubicin (dox), liposomal doxorubicin Caelyx®, H2S-releasing doxorubicin (Sdox), liposomal Sdox (Lsdox) or hyaluronated liposomal Sdox (HA-Lsdox). When indicated, 100 μM of hydroxycobalamin (Cbl), a H2S scavenger, was co-incubated. a. Pgp was isolated by immunoprecipitation from microsomal extracts; the amount of sulfhydrated Pgp was measured fluorimetrically in triplicates. Data are means ± SD (n = 5 independent experiments). *$p < 0.01$: treated vs. respective untreated (ctrl) cells; °$p < 0.001$: Cbl-treated cells vs. corresponding Cbl-untreated cells; #$p < 0.001$: Sdox/Lsdox/HA-Lsdox vs. dox/Caelyx®; §$p < 0.001$: HALsdox vs. Sdox; ◊$p < 0.001$: HA-Lsdox vs. Lsdox. b. Pgp ATPase activity was measured spectrophotometrically in triplicates, on Pgp isolated by immunoprecipitation from microsomal extracts. Data are means ± SD (n =5 independent experiments). *$p < 0.01$: treated vs. respective untreated (ctrl) cells; °$p < 0.001$: Cbl-treated cells vs. corresponding Cbl-untreated cells; #$p < 0.001$: Sdox/Lsdox/HA-Lsdox vs. dox/Caelyx®; §$p < 0.002$: HA-Lsdox vs. Sdox; ◊$p < 0.002$: HA-Lsdox vs. Lsdox. c. Ubiquitinated Pgp, isolated by immunoprecipitation from microsomal extracts, measured by a chemiluminescense-based assay in triplicates. Data are means ± SD (n = 5 independent experiments). *$p < 0.01$: treated vs. respective untreated (ctrl) cells; °$p < 0.001$: Cbl-treated cells vs. corresponding Cbl-untreated cells; #$p < 0.001$: Sdox/Lsdox/HA-Lsdox vs. dox/Caelyx®; §$p < 0.002$: HA-Lsdox vs. Sdox; ◊$p < 0.002$: HA-Lsdox vs. Lsdox. d. Microsomal proteins were immunoprecipitated (IP) with an anti-Pgp antibody, then immunoblotted (IB) with an anti-mono/poly-ubiquitin (UQ) antibody. An aliquot of the samples before immunoprecipitation was probed with an anti-Pgp antibody or with an anti-calreticulin antibody, used as control of equal protein loading. no Ab: untreated cell lysate immunoprecipitated in the absence of antibody, to check the specificity of the procedure. MW: molecular weight. The figure is representative of 1 out of 4 experiments.

## 4. Discussion

In this work, we evaluated the efficacy of HA-conjugated liposomes encapsulating Sdox against preclinical models of osteosarcoma, expressing Pgp and HA receptor CD44. These features make our models insensitive to dox and to its liposomal formulation Caelyx®, but potentially targetable by HA-conjugated nanoparticles. According to the physico-chemical features, HA-Lsdox had narrow and homogeneous size distribution, and efficient entrapment of Sdox.

The presence of HA on liposome surface did not influence their physicochemical characteristics. The DSC thermograms indicated a strong insertion of Sdox within the DSPC membrane. Such insertion protected Sdox from rapid and undesired degradation process that occurs at physiological conditions on free Sdox [15]. All these properties were maintained over time, suggesting that our formulations were stable and improved Sdox solubility and stability in physiological media.

Since HA is highly abundant in the extracellular matrix (ECM) of sarcomas, and in many tumors it serves as a reservoir of growth factors and nutrients allowing their controlled delivery to tumor cells [35], we exploited the presence of HA on the surface of Sdox-carrying liposomes, in order to enhance the homing of liposomes to osteosarcoma ECM and the subsequent intratumor delivery of their cargo. Notwithstanding the increasing use of liposomes and nanoparticles in osteosarcoma treatments [36–41], we were the first ones to validate a liposome-based treatment effective against dox-resistant/Pgp-overexpressing cells and xenografts. Of note, cells derived from the tumors either before and after the treatments displayed the same chemosensitivity profile to Sdox and its liposomal formulations than parental/chemonaíve cells. These data suggest that the tumors did not acquire a secondary resistance to Sdox, LSdox and HA-LSdox during the treatment.

In all the in vitro experiments, the maximal delivery of Sdox within whole cells and ER was reached by HA-Lsdox: this trend can be due to the higher presence of CD44 on dox-resistant cells surface, a feature that may favor the receptor-driven uptake of Sdox, and/or to the decreased efflux of Sdox via Pgp [15,16].

We recently reported that Sdox is peculiarly accumulated within ER [16]. Here, the massive release of H2S sulfhydrated nascent proteins, increased their misfolding and induced a UPR-mediated cell death.

Sdox was effective in U-2OS and Saos-2-derived sublines with increased levels of Pgp because the increased dox-resistance was paralleled by the increasing inefficiency of ERAD/ERQC system. By augmenting the burden of misfolded proteins within ER lumen, Sdox overcame the buffering capacity of the defective ERAD/ERQC system in resistant cells, triggering a ER stress-dependent cell death in cells refractory to dox [16]. This mechanism was exerted also by the liposomal formulations of Sdox, either in murine or human resistant osteosarcomas. Indeed, notwithstanding the compensatory up-regulation of ERAD/ERQCrelated genes in cells treated with HA-Lsdox, such attempt was not sufficient to rescue a proper folding of ER-associated proteins, but led to a significant ER-associated protein ubiquitination and cell death.

We previously demonstrated that in chemosensitive cells dox increases the activation of the ER stress-sensitive pro-apoptotic isoform of C/EBP-β (i.e. C/EBP-β LIP) and downstream effectors CHOP and TRB3 [42,43], and up-regulates PUMA that in turns activates caspases 12/7/3 [16,44,45]. These mechanisms occurred in Sdox-treated cells and were triggered by the release of H2S within ER lumen, as demonstrated by the absent sulfhdyration and ubiquitination of ER-associated proteins in the presence of a H2S scavenger. In all the experimental setting either in vitro or in vivo, HA-Lsdox was more effective than free Sdox and LSdox, as a consequence of the maximal drug delivery within ER achieved by this formulation.

Chemoresistant cells are usually refractory to ER stressing agents including chemotherapeutic drugs, but genetic or pharmacologic tools able to re-activate the C/EBP-β LIP/CHOP cascade re-instates a strong sensitivity to ER stress-mediated cell death [42,43,46]. The silencing of CHOP in our model indicated that this protein was the deus ex-machina of ER-dependent apoptosis in osteosarcoma, as observed in other tumors [45–47].

Besides inducing a ER stress-dependent apoptotis, HA-LSdox killed resistant cells by preventing the efflux of dox via Pgp, a protein that is markedly sulfhydrated in HA-Lsdox-treated cells.

Sulfhydration can activate or inhibit the target proteins [48]. During the folding, Pgp forms disulfide bonds that are critical to maintain a proper tertiary structure, stability and catalytic activity [49,50]. Our findings suggest that sulfhydration destabilized Pgp and promoted its degradation, in both murine and human cells. These results may explain the greater intracellular retention of Sdox formulations and the lower Vmax of Sdox efflux previously observed in U-2OS/DX580 cells [15], suggestive of a decreased amount of Pgp.

In summary, we propose an effective and safe formulation against Pgp-overexpressing/dox-resistant osteosarcoma. The greater efficacy of HA-Lsdox relies on increased intracellular uptake, decreased efflux because of Pgp degradation, increased cell death triggered by ER stress.

All these features were coupled with low cardiotoxic and systemic toxicity profile. Given the high inter-patients variability and heterogeneity of osteosarcomas, we are aware that our results, obtained in one

human and one murine resistant cell line of osteosarcoma, cannot be generalized bona fide to all chemoresistant osteosarcomas. Our results indicate, however, that the efficacy of HA-Lsdox was not cell-specific or species-specific. If such efficacy will be confirmed in a larger cohort of resistant osteosarcoma cell lines or primary cells, we may propose HALsdox as an innovative tool for clinical settings, in particular in osteosarcoma patients with high levels of Pgp and resistance to doxorubicin, where the rate of failure of the first-line chemotherapy is high.

**Declarations of interest**

None.

**Acknowledgments**

This work was supported by the Italian Association for Cancer Research (AIRCS; IG15232, IG21408), by the Italian Ministry of University and Research (Future in Research Project 2012, RBFR12SOQ1; FARB2017) and by Italian Ministry for University and Research (MIUR)—University of Torino, "Fondi Ricerca Locale (ex-60%)".

We thanks Mr. Costanzo Costamagna, Department of Oncology, University of Torino, Italy, for the technical assistance.

**Appendix A.** Supplementary data

Supplementary data to this article can be found online at https://doi.org/10.1016/j.canlet.2019.04.029

References

[1] S. Ferrari, M. Serra, An update on chemotherapy for osteosarcoma, Expert Opin.Pharmacother. 16 (2015) 2727–2736, https://doi.org/10.1517/14656566.2015.1102226.

[2] C.M. Hattinger, M. Fanelli, E. Tavanti, S. Vella, S. Ferrari, P. Picci, M. Serra,Advances in emerging drugs for osteosarcoma, Expert Opin. Emerg. Drugs 20 (2015) 495–514 0.1517/14728214.2015.1051965.

[3] C.M. Hattinger, M. Fanelli, E. Tavanti, S. Vella, C. Riganti, P. Picci, M. Serra, Doxorubicin-resistant osteosarcoma: novel therapeutic approaches in sight? Future Oncol. 13 (2017) 673–677, https://doi.org/10.2217/fon-2016-0519.

[4] M.M. Gottesman, T. Fojo, S.E. Bates, Multidrug resistance in cancer: role of ATPdependent transporters, Nat. Rev. Canc. 2 (2002) 48–58 0.1038/nrc706.

[5] M. Fanelli, C.M. Hattinger, S. Vella, E. Tavanti, F. Michelacci, B. Gudeman, D. Barnett, P. Picci, M. Serra, Targeting ABCB1 and ABCC1 with their Specific Inhibitor CBT-1® can overcome drug resistance in osteosarcoma, Curr. Cancer Drug Targets 16 (2016) 261–274, https://doi.org/10.2174/1568009616666151106120434.

[6] N. Baldini, K. Scotlandi, G. Barbanti-Brodano, M.C. Manara, D. Maurici, G. Bacci, F. Bertoni, P. Picci, S. Sottili, M. Campanacci Serra, Expression of P-glycoprotein in high-grade osteosarcomas in relation to clinical outcome, N. Engl. J. Med. 23 (1995) 1380–1385, https://doi.org/10.1056/NEJM199511233332103.

[7] H.S. Chan, T.M. Grogan, G. Haddad, G. DeBoer, V. Ling, P-glycoprotein expression: critical determinant in the response to osteosarcoma chemotherapy, J. Natl. Cancer Inst. 19 (1997) 1706–1715, https://doi.org/10.1093/jnci/89.22.1706.

[8] E.E. Pakos, J.P. Ioannidis, The association of P-glycoprotein with response to chemotherapy and clinical outcome in patients with osteosarcoma. A meta-analysis, Cancer 98 (2003) 581–589, https://doi.org/10.1002/cncr.11546.

[9] M. Serra, K. Scotlandi, G. Reverter-Branchat, S. Ferrari, M.C. Manara, S. Benini, M. Incaprera, F. Bertoni, M. Mercuri, A. Briccoli, G. Bacci, P. Picci, Value of Pglycoprotein and clinicopathologic factors as the basis for new treatment strategies in high-grade osteosarcoma of the extremities, J. Clin. Oncol. 21 (2003) 536–542, https://doi.org/10.1200/JCO.2003.03.144.

[10] S.E. Lipshultz, R. Karnik, P. Sambatakos, V.I. Franco, S.W. Ross, T.L. Miller, Anthracycline-related cardiotoxicity in childhood cancer survivors, Curr. Opin. Cardiol. 29 (2014) 103–112, https://doi.org/10.1097/HCO.0000000000000034.

[11] K.M. Skubitz, Phase II trial of pegylated-liposomal doxorubicin (Doxil) in sarcoma, Canc. Invest. 21 (2003) 167–176.

[12] R. De Sanctis, A. Bertuzzi, U. Basso, A. Comandone, S. Marchetti, A. Marrari, P. Colombo, R.F. Lutman, L. Giordano, A. Santoro, Non-pegylated liposomal doxorubicin plus ifosfamide in metastatic soft tissue sarcoma: results from a phase-II trial, Anticancer Res. 35 (2015) 543–547.
[13] A. Gabizon, Y. Patil, N.M. La-Beck, New insights and evolving role of Pegylated liposomal doxorubicin in cancer therapy, Drug Resist. Updates 29 (2016) 90–106, https://doi.org/10.1016/j.drup.2016.10.003.
[14] E. Gazzano, B. Rolando, K. Chegaev, I.C. Salaroglio, J. Kopecka, I. Pedrini, S. Saponara, M. Sorge, I. Buondonno, B. Stella, A. Marengo, M. Valoti, M. Brancaccio, R. Fruttero, A. Gasco, S. Arpicco, C. Riganti, Folate-targeted liposomal nitrooxy-doxorubicin: an effective tool against P-glycoprotein-positive and folate receptor-positive tumors, J. Control. Release 270 (2018) 37–52, https://doi.org/10.1016/j.jconrel.2017.11.042.
[15] K. Chegaev, B. Rolando, D. Cortese, E. Gazzano, I. Buondonno, L. Lazzarato, M. Fanelli, C.M. Hattinger, M. Serra, C. Riganti, R. Fruttero, D. Ghigo, A. Gasco, H2S-donating doxorubicins may overcome cardiotoxicity and multidrug resistance, J. Med. Chem. 59 (2016) 4881–4889, https://doi.org/10.1021/acs.jmedchem.6b00184.
[16] I. Buondonno, E. Gazzano, E. Tavanti, K. Chegaev, J. Kopecka, M. Fanelli, B. Rolando, R. Fruttero, A. Gasco, C. Hattinger, M. Serra, C. Riganti, Endoplasmic reticulum-targeting doxorubicin: a new tool effective against doxorubicin-resistant osteosarcoma, Cell. Mol. Life Sci. 76 (2019) 609–625, https://doi.org/10.1007/s00018-018-2967-9.
[17] E. Bigagli, C. Luceri, M. De Angioletti, K. Chegaev, M. D'Ambrosio, C. Riganti, E. Gazzano, S. Saponara, M. Longini, F. Luceri, L. Cinci, New NO- and H2S-releasing doxorubicins as targeted therapy against chemoresistance in castration-resistant prostate cancer: in vitro and in vivo evaluations, Investig. New Drugs 36 (2018) 985–998, https://doi.org/10.1007/s10637-018-0590-0.
[18] E. Boldrini, S.V. Peres, S. Morini, B. de Camargo, Immunoexpression of Ezrin and CD44 in patients with osteosarcoma, J. Pediatr. Hematol. Oncol. 32 (2010) e213–217, https://doi.org/10.1097/MPH.0b013e3181e5e247.
[19] A. Gvozdenovic, M.J. Arlt, C. Campanile, P. Brennecke, K. Husmann, W. Born, R. Muff, B. Fuchs, Silencing of CD44 gene expression in human 143-B osteosarcoma cells promotes metastasis of intratibial tumors in SCID mice, PLoS One 8 (2013) e60329, , https://doi.org/10.1371/journal.pone.0060329.
[20] A. Gvozdenovic, M.J. Arlt, C. Campanile, P. Brennecke, K. Husmann, Y. Li, W. Born, R. Muff, B. Fuchs, CD44 enhances tumor formation and lung metastasis in experimental osteosarcoma and is an additional predictor for poor patient outcome, J. Bone Miner. Res. 28 (2013) 838–847, https://doi.org/10.1002/jbmr.1817.
[21] Y. Gao, Y. Feng, J.K. Shen, M. Lin, E. Choy, G.M. Cote, D.C. Harmon, H.J. Mankin, F.J. Hornicek, Z. Duan, CD44 is a direct target of miR-199a-3p and contributes to aggressive progression in osteosarcoma, Sci. Rep. 5 (2015) e11365, , https://doi. org/10.1038/srep11365.
[22] T. Liu, Z. Yan, Y. Liu, E. Choy, F.J. Hornicek, H. Mankin, Z. Duan, CRISPR-Cas9-mediated silencing of CD44 in human highly metastatic osteosarcoma cells, Cell. Physiol. Biochem. 4 (2018) 1218–1230, https://doi.org/10.1.115599/0/000484980970272.
[23] L. Mayr, C. Pirker, D. Lötsch, S. Van Schoonhoven, R. Windhager, B. Englinger, W. Berger, B. Kubista, CD44 drives aggressiveness and chemoresistance of a metastatic human osteosarcoma xenograft model, Oncotarget 8 (2017) 114095–114108, https://doi.org/10.18632/oncotarget.23125.
[24] S. Arpicco, C. Lerda, E. Dalla Pozza, C. Costanzo, N. Tsapis, B. Stella, M. Donadelli, I. Dando, E. Fattal, L. Cattel, M. Palmieri, Hyaluronic acid-coated liposomes for active targeting of gemcitabine, Eur. J. Pharm. Biopharm. 85 (2013) 373–380, https://doi.org/10.1016/j.ejpb.2013.06.003.
[25] G.R. Bartlett, Phosphorus assay in column chromatography, J. Biol. Chem. 234 (1959) 466–468.
[26] I. Pedrini, E. Gazzano, K. Chegaev, B. Rolando, A. Marengo, J. Kopecka, R. Fruttero, D. Ghigo, S. Arpicco, C. Riganti, Liposomal nitrooxy-doxorubicin: one step over Caelyx® in drug-resistant human cancer cells, Mol. Pharm. 11 (2014) 3068–3079, https://doi.org/10.1021/mp500257s.
[27] M. Serra, K. Scotlandi, M.C. Manara, D. Maurici, P.L. Lollini, C. De Giovanni, G. Toffoli, N. Baldini, Establishment and characterization of multidrug-resistant human osteosarcoma cell lines, Anticancer Res. 13 (1993) 323–329.
[28] C. Riganti, E. Miraglia, D. Viarisio, C. Costamagna, G. Pescarmona, D. Ghigo, A. Bosia, Nitric oxide reverts the resistance to doxorubicin in human colon cancer cells by inhibiting the drug efflux, Cancer Res. 65 (2005) 516–525.

[29] C. Riganti, B. Rolando, J. Kopecka, I. Campia, K. Chegaev, L. Lazzarato, A. Federico, R. Fruttero, D. Ghigo, Mitochondrial-targeting nitrooxy-doxorubicin: a new approach to overcome drug resistance, Mol. Pharm. 10 (2013) 161–174, https://doi.org/10.1021/mp300311b.
[30] M. De Acetis, A. Notte, F. Accornero, G. Selvetella, M. Brancaccio, C. Vecchione, M. Sbroggiò, M. Collino, D. Pacchioni, G. Lanfranchi, A. Aretini, R. Ferretti, A. Maffei, F. Altruda, L. Silengo, G. Tarone, G. Lembo, Cardiac overexpression of melusin protects from dilated cardiomyopathy due to long-standing pressure overload, Circ. Res. 27 (2005) 1087–1094, https://doi.org/10.1161/01.RES.0000168028.36081.e0.
[31] N. Sen, B.D. Paul, M.M. Gadalla, A.K. Mustafa, T. Sen, R. Xu, S. Kim, S.H. Snyder, Hydrogen sulfide-linked sulfhydration of NF-κB mediates its antiapoptotic actions, Mol. Cell. 45 (2012) 13–24, https://doi.org/10.1016/j.molcel.2011.10.021.
[32] J. Kopecka, G. Salzano, I. Campia, S. Lusa, D. Ghigo, G. De Rosa, C. Riganti, Insights in the chemical components of liposomes responsible for P-glycoprotein inhibition, Nanomedicine 10 (2014) 77–87, https://doi.org/10.1016/j.nano.2013.06.013.
[33] C. Hetz, The unfolded protein response: controlling cell fate decisions under ER stress and beyond, Nat. Rev. Mol. Cell Biol. 13 (2012) 89–102 https://doi.org/10.1038/nrm3270.
[34] E. Chevet, C. Hetz, A. Samali, Endoplasmic reticulum stress-activated cell reprogramming in oncogenesis, Cancer Discov. 5 (2015) 586–597, https://doi.org/10.1158/2159-8290.
[35] M.F. Brizzi, G. Tarone, P. Defilippi, Extracellular matrix, integrins, and growth factors as tailors of the stem cell niche, Curr. Opin. Cell Biol. 24 (2012) 645–651, https://doi.org/10.1016/j.ceb.2012.07.001.
[36] N. Federman, J. Chan, J.O. Nagy, E.M. Landaw, K. McCabe, A.M. Wu, T. Triche, H. Kang, B. Liu, J.D. Marks, C.T. Denny, Enhanced growth inhibition of osteosarcoma by cytotoxic polymerized liposomal nanoparticles targeting the alcam cell surface receptor, Sarcoma 2012 (2012) e126906, , https://doi.org/10.1155/2012/126906.
[37] L. Eikenes, M. Tari, I. Tufto, O.S. Bruland, C. de Lange Davies, Hyaluronidase induces a transcapillary pressure gradient and improves the distribution and uptake of liposomal doxorubicin (Caelyx) in human osteosarcoma xenografts, Br. J. Canc.93 (2005) 81–88.
[38] D. Wu, M. Wan, Methylene diphosphonate-conjugated adriamycin liposomes: preparation, characteristics, and targeted therapy for osteosarcomas in vitro and in vivo, Biomed. Microdevices 14 (2012) 497–510, https://doi.org/10.1007/s10544-011-9626-3.
[39] F. Haghiralsadat, G. Amoabediny, S. Naderinezhad, K. Nazmi, J.P. De Boer, B. Zandieh-Doulabi, T. Forouzanfar, M.N. Helder, EphA2 Targeted doxorubicinnanoliposomes for osteosarcoma treatment, Pharm. Res. (N. Y.) 34 (2017) 2891–2900, https://doi.org/10.1007/s11095-017-2272-6.
[40] F. Haghiralsadat, G. Amoabediny, M.H. Sheikhha, B. Zandieh-Doulabi, S. Naderinezhad, M.N. Helder, T. Forouzanfar, New liposomal doxorubicin nanoformulation for osteosarcoma: drug release kinetic study based on thermo and pH sensitivity, Chem. Biol. Drug Des. 90 (2017) 368–379, https://doi.org/10.1111/cbdd.12953.
[41] Y. Chi, X. Yin, K. Sun, S. Feng, J. Liu, D. Chen, C. Guo, Z. Wu, Redox-sensitive and hyaluronic acid functionalized liposomes for cytoplasmic drug delivery to osteosarcoma in animal models, J. Control. Release 261 (2017) 113–125, https://doi.org/10.1016/j.jconrel.2017.06.027.
[42] C. Riganti, J. Kopecka, E. Panada, S. Barak, M. Rubinstein, The role of C/EBP-β LIP in multidrug resistance, J. Natl. Cancer Inst. 107 (2015), https://doi.org/10.1093/jnci/djv046 djv046.
[43] J. Kopecka, I.C. Salaroglio, L. Righi, R. Libener, S. Orecchia, F. Grosso, V. Milosevic, P. Ananthanarayanan, L. Ricci, E. Capelletto, M. Pradotto, F. Napoli, M. Di Maio, S. Novello, M. Rubinstein, G.V. Scagliotti, C. Riganti, Loss of C/EBP-β LIP drives cisplatin resistance in malignant pleural mesothelioma, Lung Canc. 120 (2018) 34–45, https://doi.org/10.1016/j.lungcan.2018.03.022.
[44] J. Li, B. Lee, A.S. Lee, Endoplasmic reticulum stress-induced apoptosis: multiple pathways and activation of p53-up-regulated modulator of apoptosis (PUMA) and NOXA by p53, J. Biol. Chem. 281 (2006) 7260–7270, https://doi.org/10.1074/jbc.M509868200.
[45] S.C. Cazanave, N.A. Elmi, Y. Akazawa, S.F. Bronk, J.L. Mott, G.J. Gores, CHOP and AP-1 cooperatively mediate PUMA expression during lipoapoptosis, Am. J. Physiol. Gastrointest. Liver Physiol. 299 (2010) G236–G243, https://doi.org/10.1152/ajpgi.00091.2010.

[46] I.C. Salaroglio, E. Gazzano, A. Abdullrahman, E. Mungo, B. Castella, G.E.F. Abdellatef Abd-elrahman, M. Massaia, M. Donadelli, M. Rubinstein, C. Riganti, J. Kopecka, Increasing intratumor C/EBP-β LIP and nitric oxide levels overcome resistance to doxorubicin in triple negative breast cancer, J. Exp. Clin. Cancer Res.(2018), https://doi.org/10.1186/s13046-018-0967-0.
[47] C. Chiribau, F. Gaccioli, C. Huang, C. Yuan, M. Hatzoglou, Molecular symbiosis of chop and c/ebp beta isoform lip contributes to endoplasmic reticulum stress-induced apoptosis, Mol. Cell Biol. 30 (2010) 3722–3731, https://doi.org/10.1128/MCB.01507-09.
[48] L. Li, P. Rose, P.K. Moore, Hydrogen sulfide and cell signaling, Annu. Rev. Pharmacol. Toxicol. 51 (2011) 169–187, https://doi.org/10.1146/annurevpharmtox-010510-100505.
[49] D.J. Swartz, L. Mok, S.K. Botta, A. Singh, G.A. Altenberg, I.L. Urbatsch, Directed evolution of P-glycoprotein cysteines reveals site-specific, non-conservative substitutions that preserve multidrug resistance, Biosci. Rep. 34 (2014) e00116, https://doi.org/10.1042/BSR20140062.
[50] L. Pan, S.G. Aller, Equilibrated atomic models of outward-facing P-glycoprotein and effect of ATP binding on structural dynamics, Sci. Rep. 5 (2015) e7880, , https://doi.org/10.1038/srep07880.